THE JOURNAL OF PHYSICAL CHEMISTRY C
A JOURNAL OF THE AMERICAN CHEMICAL SOCIETY

pubs.acs.org/JPCC

Article

Steering the Selectivity in Gold–Titanium-Catalyzed Propene Oxidation by Controlling the Surface Acidity

Ewoud J.J. de Boed, Jan Willem de Rijk, Petra E. de Jongh, and Baira Donoeva*

Cite This: *J. Phys. Chem. C* 2021, 125, 16557–16568

Read Online

ABSTRACT: Supported nanoparticulate Au/Ti-SiO_2 catalysts are a promising candidate for selective epoxidation of propene with H_2/O_2 mixtures. Here, we demonstrate that by altering the acidity of the surface titanol groups in Au/Ti-SiO_2, the selectivity of these catalysts in propene oxidation can be controlled. That is, Au/Ti-SiO_2 prepared using an alkali base during gold deposition shows basic properties due to the formation of Ti-ONa groups. The catalysts that contained Na^+ and neutralized acid sites demonstrate high selectivity toward propene oxide. On the contrary, when the acidity of the Ti-OH groups is preserved by using NH_4OH as a base during gold deposition, the catalyst is highly selective toward propanal at a similar propene conversion. This difference in selectivity is explained by the isomerization of initially formed propene oxide into propanal over acidic Ti-OH groups as we demonstrated using stacked bed experiments, where the Ti-support was exposed to propene oxide. When Na^+ was present, no isomerization was observed, while without Na^+ present, propene oxide was isomerized to propanal. In short, we demonstrate the crucial role of Na^+ and acidic Ti-sites in steering the selectivity in gold-catalyzed propene epoxidation.

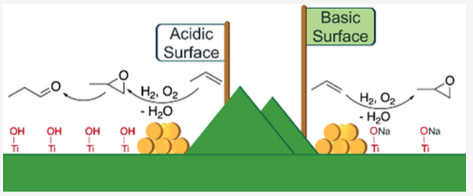

INTRODUCTION

Selective oxidation of alkenes is of major industrial importance.[1] Oxygenates of simple alkenes find end-user application in various polymers. In the E.U., more than 13% of propene is converted into propene oxide (PO).[2] For ethene oxide (EO) production, primarily supported silver catalysts are used. While Ag/Al_2O_3 catalyzes the direct oxidation of ethene with molecular oxygen, their use for propene oxidation results in complete oxidation.[3,4] Instead, PO is produced via indirect oxidation processes: oxidation of propene with hydroperoxides and the so-called chlorohydrin route (Scheme 1).[5] The chlorohydrin route is the older process. In this process, propene is chlorinated to propene chlorohydrin and subsequently dehydrochlorinated with $Ca(OH)_2$ to produce propene oxide and $CaCl_2$.[3−5] It has an environmental disadvantage since it produces chlorinated hydrocarbons and an equal molar amount of $CaCl_2$ as waste. Alternatively, the hydroperoxide route is based on the epoxidation of propene with various hydroperoxides catalyzed by heterogeneous Ti-catalysts or homogeneous Mo-catalysts. This route, however, couples the production of propene oxide to other bulk chemicals, such as methyl-*tert*-butyl-ether (in the *tert*-butylhydroperixode process) or styrene (in the styrene monomer-propene oxide process). Alternatively, it relies on the use of H_2O_2 in the hydrogen peroxide propene oxide (HPPO) process or hydrogen peroxide route, which carries high raw material costs and has safety disadvantages due to a high concentration of the oxidant.[3−7]

Other potential products of propene oxidation, such as propanal, are also valuable. Propanal is currently produced using hydroformylation of ethene with CO over a homogeneous Rh-catalyst.[8,9]

An alternative route for PO production with easy catalyst separation, limited environmental impact, and high reactant efficiency is highly desirable. A candidate is the direct gas-

Scheme 1. Routes for Industrial Propene Epoxidation

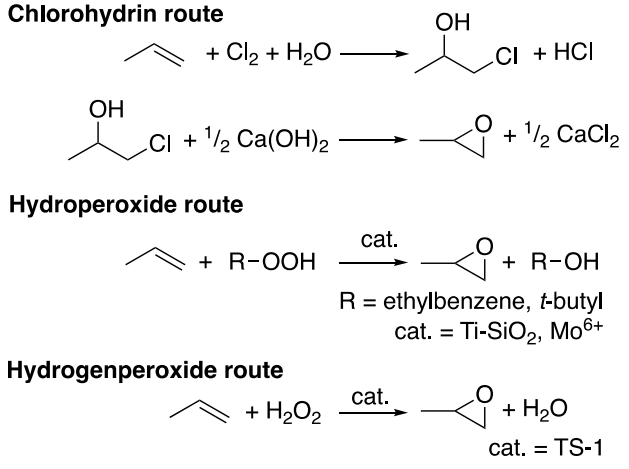

Received: June 23, 2021
Revised: July 15, 2021
Published: July 27, 2021

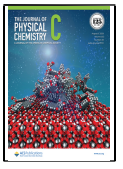

https://doi.org/10.1021/acs.jpcc.1c05503
J. Phys. Chem. C 2021, 125, 16557−16568

phase oxidation of propene with H_2/O_2 mixtures over nanoparticular gold-based catalysts. As first shown by Haruta *et al.*, titania supported gold nanoparticles of 2−5 nm catalyzed epoxidation of propene with H_2/O_2 at conversions of <1% propene, with >99% selectivity to PO.[10,11]

Since then, research has contributed to the understanding of the reaction mechanism and improvement of the epoxidation of propene over gold−titanium(IV)-based catalysts. The proposed mechanism (Scheme 2) consists of two main steps:

Scheme 2. Mechanism of Propene Epoxidation over Au−Ti Catalysts, Adapted from Haruta *et al.*[12]

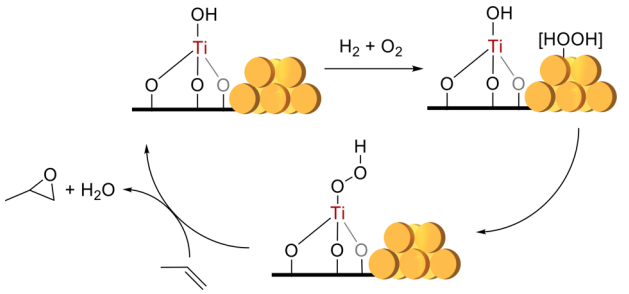

first, a hydroperoxide is formed from H_2/O_2 over the surface of small (<5 nm) gold nanoparticles[13] followed by its spillover to form Ti-OOH,[12] which transfers the electrophilic oxygen to the C=C bond, offering PO with high selectivity.[14] This mechanism is supported by spectroscopic experiments by Oyama *et al.*, who detected Ti-OOH as an intermediate.[12] Whether the active sites are neighboring Au−Ti sites or interfacial Au−Ti sites is still under debate.[13,15]

At first, TiO_2 was used as a support for gold nanoparticles. However, the Au/TiO_2 catalysts lost their activity in the course of hours due to irreversible adsorption of propoxy-species,[16,17] and the presence of Ti-O-Ti oligomers on silica-supported catalysts favored complete oxidation of propene to CO_2.[15] A high dispersion of titanium(IV) sites on an inert silica surface was soon shown to improve both catalyst stability and selectivity in propene epoxidation with H_2/O_2 mixtures.[11,18]

Only small (<5 nm) supported gold nanoparticles prepared via deposition precipitation (DP) lead to active and selective catalysts for propene epoxidation, whereas Au−Ti catalysts prepared via impregnation give total propene oxidation and propene hydrogenation.[11] Severe propene hydrogenation is sometimes also observed for small (<6 nm) supported gold nanoparticles.[19,20] Other oxygenates such as acrolein, acetone, propanal, and ethanal are typically only observed in trace amounts. Delgass *et al.* demonstrated the effect of different preparation methods for Au−Ti-based catalysts in propene epoxidation. The group showed that the titanium(IV) dispersion had a large impact on catalyst performance.[21] Haruta *et al.* demonstrated that alkali hydroxides were necessary in propene oxidation over small supported gold clusters with O_2/H_2O instead of O_2/H_2.[22] It was speculated that under those conditions, alkali salts interacted with the gold cluster to activate O_2 and, after the reaction with H_2O, formed peroxide. However, the use of H_2O instead of H_2 leads to an increased acrolein selectivity due to the preferred O insertion at the allylic C−H.

Haruta and co-workers showed that the presence of alkali cations on the catalyst suppressed the propene hydrogenation activity during propene epoxidation. They postulated that trace amounts of Na^+ and K^+ lead to the generation of more oxygen vacancies on the Ti-based oxidic support. This promotor effect was only observed for gold nanoparticles of 2−5 nm. Both smaller and larger particles catalyzed mainly propene hydrogenation.[20] Nijhuis and co-workers elaborated on the oxidation of propene with water and oxygen and demonstrated that alkali ions enhance the gold uptake from the precursor solution during catalyst preparation.[23] In addition, they showed that the prepared Au/TS-1 catalysts produced acrolein as the major reaction product. It was observed that the acrolein formation rate for different gold catalysts did not change in the presence or absence of titanium(IV). It was postulated that acrolein is formed over Au-sites that are incapable of forming peroxide.[23] Until now, a systematic study on the influence of Na^+ on the acidity and selectivity of Au/Ti-SiO_2 catalysts in propene epoxidation has not been performed.

In this study, well-defined site-isolated titanium(IV)-grafted silica was decorated with small gold nanoparticles. The gold nanoparticles were introduced via cation adsorption using different gold precursor/base combinations. Catalysts with different acid/base properties were prepared, and we clearly demonstrate the crucial role of the acid/base properties of the Ti-sites on the selectivity in propene oxidation with H_2/O_2 mixtures.

METHODS

Chemicals. All chemicals were used as received without further purification: bis(cyclopentadienyl)titanium dichloride (STREM, 99+%, stored in an Ar glovebox), chloroform (Acros Organics, anhydrous, 99.9%), 1,2-dichloroethane (Acros Organics, anhydrous, 99.8%), $HAuCl_4 \cdot 3H_2O$ (Acros Organics, reagent ACS, ≥49.0% Au), silica (SiO_2, GRACE SI 1404, BET S.A. 525 m^2/g, P.D. 7.4 nm, P.V. 0.92 cm^3/g was kindly provided by GRACE), and triethylamine (Sigma-Aldrich, anhydrous, ≥99.5%).

General Considerations. For inert preparations, common Schlenk techniques and equipment were used using glassware with Teflon joints. All preparations involving gold were performed in the absence of light in glassware cleaned with aqua regia prior to use.

Grafting of Titanium. Titanium(IV) sites were grafted onto a silica surface using titanocene dichloride using an adapted literature procedure.[24] In brief, 2.0 g of previously dried SiO_2 was dispersed in 20 mL of anhydrous 1,2-dichloroethane under a N_2 atmosphere. To this suspension, an appropriate amount of bis(cyclopentadienyl)-titanium dichloride in a 1,2-dichloroethane solution was added corresponding to 0.10 or 0.50 metal sites per nm^2 (nominal 0.4 and 2.0 wt % Ti). The red mixture was stirred at 60 °C for 1 h to allow for diffusion of the metallocene into the pores. This was followed by the addition of 2.0 mL of anhydrous triethylamine at room temperature and subsequent heating at 60 °C for 3 h. The grafted *x*TiCp-SiO_2 was recovered *via* filtration, washed three times with plenty of anhydrous chloroform, dried *in vacuo*, and calcined in static air at 500 °C for 4 h, ramp 10 °C/min to offer titanium(IV)-grafted silica denoted as *x*Ti-SiO_2, with *x* corresponding to the nominal surface density in atoms/nm^2 derived from the titanium loading as evidenced from elemental analysis and the Brunauer−Emmett−Teller (BET) surface area from N_2 physisorption (Figure S1).

Preparation of Supported Gold Nanoparticles from $Au(en)_2Cl_3$. As described by Dai *et al.*,[25] 1.0 g of 0.5Ti-SiO_2

https://doi.org/10.1021/acs.jpcc.1c05503
J. Phys. Chem. C 2021, 125, 16557−16568

and the appropriate amount of previously synthesized $Au(en)_2Cl_3$[26] (4.04 mg; corresponding to 0.20 wt % Au) were dispersed in 50 mL of Milli-Q water. Under vigorous stirring, the pH was raised from 4.6 to 9.6 by addition of an aqueous 2.5 wt % Na_2CO_3 solution. The reaction was allowed to continue for 3 h in the dark. The solids were collected over a glass filter and washed with 20 mL of Milli-Q water four times until $AgNO_3$ addition did not show the formation of a precipitate. The white solids were allowed to dry at room temperature in the dark, subsequently reduced at 300 °C (2 h, 50 mL/min, 20% H_2 in N_2, ramp 5 °C/min), and calcined at 450 °C in artificial air for 3 h (ramp 10 °C/min) to offer a pink powder denoted as Au/xTi-SiO_2 (Na_2CO_3).

Preparation of Supported Gold Nanoparticles from $HAuCl_4 \cdot 3H_2O$. As described by Nijhuis *et al.*,[19] 1.0 g of xTi-SiO_2 was dispersed in 50 mL of Milli-Q water followed by addition of a $HAuCl_4 \cdot 3H_2O$ solution (4.05 mg, 10 mL Milli-Q, corresponding to 0.20 wt % Au). The pH of the mixture was raised from 3.8 to 9.6 by addition of a dilute NH_4OH solution (2.5 wt %). The mixture was stirred in the dark for 1.5 h followed by retrieval of white solids via filtration. The solids were washed four times with plenty of Milli-Q water, dried at room temperature in the dark, subsequently reduced at 300 °C (2 h, 20% H_2 in N_2, 5 °C/min), and finally calcined at 400 °C in artificial air for 3 h (ramp 10 °C/min) to offer the catalysts as pink powders denoted as Au/xTi-SiO_2 (NH_4OH) all at a nominal gold loading of 0.20 wt %.

Acid Post-synthesis Treatment. Au/0.5Ti-SiO_2 (Na_2CO_3) (150 mg) was treated with 2 mL of 0.1 M HNO_3(aq), filtrated immediately, and washed three times with plenty of Milli-Q water. The powder was dried under ambient conditions in the dark and at 120 °C for 2 h. The retrieved catalyst was denoted as Au/0.5Ti-SiO_2 (Na_2CO_3 + acid).

Alkaline Post-synthesis Treatment. Au/0.5Ti-SiO_2 (NH_4OH) (200 mg) was dried *in vacuo* at 100 °C for 24 h followed by incipient wetness impregnation of 0.18 mL of a 0.25 M NaOH solution in Milli-Q, corresponding to 0.4 wt % Na^+, and drying *in vacuo* at 90 °C for 2 h to offer a pink powder, denoted as Au/0.5Ti-SiO_2 (NH_4OH + base).

Alkaline Treatment of the Support. 0.5Ti-SiO_2 (1.0 g) was dispersed in 50 mL of Milli-Q water. Under vigorous stirring, the pH was raised from 3.1 to 8.5 by addition of an aqueous 2.5 wt % Na_2CO_3 solution. The reaction was allowed to continue for 3 h. The solids were collected via centrifugation (5 min, 6000 rpm) and washed with 20 mL of Milli-Q water four times with centrifugation in between. The white solids were allowed to dry at room temperature, subsequently reduced at 300 °C (2 h, 50 mL/min, 20% H_2 in N_2, ramp 5 °C/min), and calcined at 400 °C in artificial air for 3 h (ramp 10 °C/min) to offer a white powder denoted as 0.5Ti-SiO_2 (Na_2CO_3) with a PZC of 8.1.

Catalyst Characterization. Diffuse reflectance UV−vis (DR UV−vis) was recorded under ambient conditions on a Perkin Elmer Lambda 950S coupled with a 150 mm integrating sphere and an InGaAs detector using a PTFE standard as white (200−800 nm, 4 nm interval, slit size 4 nm); the absorbance spectra obtained were corrected for Kubelka−Munk and normalized to the sole absorbance band of the pristine silica at 210 nm (more details are included in the SI). Nitrogen physisorption measurements were done at 77 K using a Micromeritics TriStar 3000. Powder XRD was performed with a Bruker D2 phaser with a Co Kα source. Elemental analysis was performed by inductively coupled plasma mass spectrometry (Geosciences, Universiteit Utrecht, The Netherlands, for Au. Ti compositions were determined at Mikroanalytisches Laboratorium Kolbe, Germany).

Fourier transform infrared spectroscopy (FTIR) was performed on a Thermoscientific Nicolet iS5 using a custom-built cell in transmission mode. Sixty-four scans were used for the background and 32 scans for samples at a resolution of 4 cm^{-1}. In brief, self-supporting pellets of approximately 20 mg (12 mm diameter) were evacuated *in vacuo* at room temperature for 1 h at *ca.* 6.0×10^{-5} mbar followed by recording the desired spectrum. Where applicable, an integrated molar extinction coefficient $\varepsilon_{(OH)}$ 3.44 was used for determination of isolated silanol concentration.[27]

Fourier transform infrared spectroscopy with adsorption and desorption of pyridine (Py-FTIR) was performed on a Thermoscientific Nicolet iS5 using a custom-built cell in transmission mode. Sixty-four scans were used for the background and 32 scans for samples at a resolution of 4 cm^{-1}. In brief, self-supporting pellets of approximately 20 mg (12 mm diameter) were evacuated at room temperature for 1 h. At 30 °C, 15 mbar of pyridine (Sigma-Aldrich, 99.8%) vapor was allowed to adsorb on the sample for 30 min, with spectra recorded every 5 min. After adsorption, the sample was evacuated for 15 min under dynamic high vacuum followed by temperature-programmed desorption of the pyridine under dynamic high vacuum (30−500 °C, ramp 5 °C/min) with spectra recorded every 25 °C. The acid concentration was determined after evacuation at 200 °C under dynamic high vacuum using the ν19b vibrations with the molar extinction coefficients as reported by Emeis ε_{1455} = 2.22 and ε_{1545} = 1.67.[27]

Transmission electron microscopy (TEM) and elemental mapping images were collected on a Talos F200X microscope operated at 200 kV. Average particle sizes were determined by counting typically 200−300 individual particles. Energy-dispersive X-ray spectroscopy (EDX) was performed by four windowless SuperX EDX-detectors with a resolution of 128 eV arranged around the sample. Identification of the EDX signal was carried out using the Velox software. The point-of-zero-charge (PZC) of the catalysts was recorded with a Radiometer analytical, MeterLab PHM210 standard pH meter. The weight loss of the spent catalyst was determined using a PerkinElmer TGA 8000 equipped with a mass spectrometer (MS) under 20% O_2 in Ar at 14 mL/min total flow.

X-ray photoelectron spectroscopy (XPS) was performed using a K-Alpha XPS spectrometer (Thermo Scientific) equipped with an Al anode (Al Kα = 1486.68 eV) monochromatized X-ray source. Powder samples were placed on a double-sided carbon tape, and the spectra were acquired using a flood-gun source to account for surface charging. A pass energy of 50 eV and spot size of 400 μm were used. The peak binding energies were calibrated against the C 1s peak at 284.8 eV. Analysis of XPS data was performed using the Casa XPS software.

Propene Oxidation with H_2/O_2 Mixtures. The oxidation of propene was performed in a quartz fixed bed reactor (internal diameter of 4 mm) loaded with 150 mg of the catalyst (sieve fraction of 90−150 μm) and diluted with SiC (300 mg, <425 μm). Prior to catalysis, the catalysts were treated under 10% H_2 in He at 250 °C for 1 h. The reaction was carried out at 200 °C with a typical gas feed of 25 mL/min in total with a volumetric concentration of 10% of each reactant (H_2, O_2, and C_3H_6) in helium as a balance at a GHSV of 10,000 mL/g_{cat}/h.

https://doi.org/10.1021/acs.jpcc.1c05503
J. Phys. Chem. C 2021, 125, 16557−16568

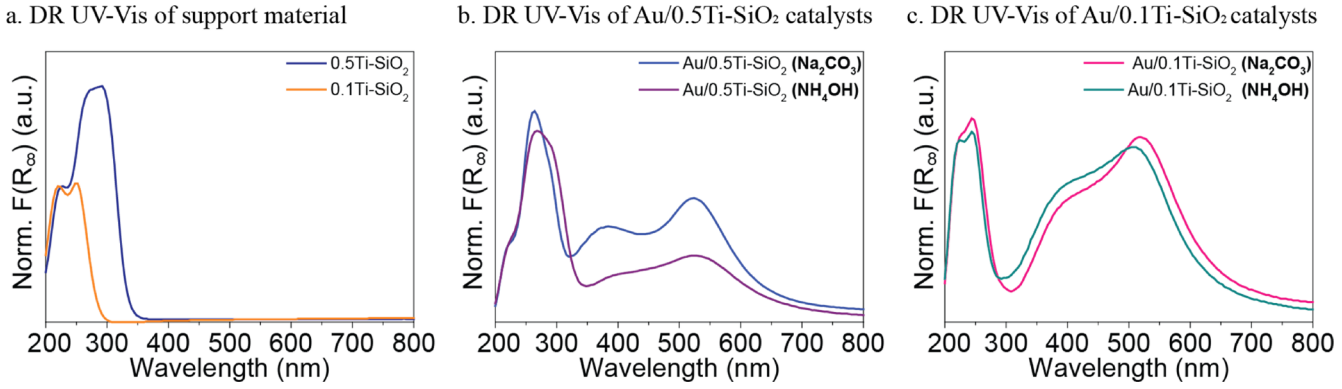

Figure 1. Support and catalyst characterizations. (a) Diffuse reflectance UV−vis absorption spectra of the *x*Ti-SiO_2 supports, (b) DR UV−vis of the Au/0.5Ti-SiO_2 catalysts, and (c) DR UV−vis of the Au/0.1Ti/SiO_2 catalysts.

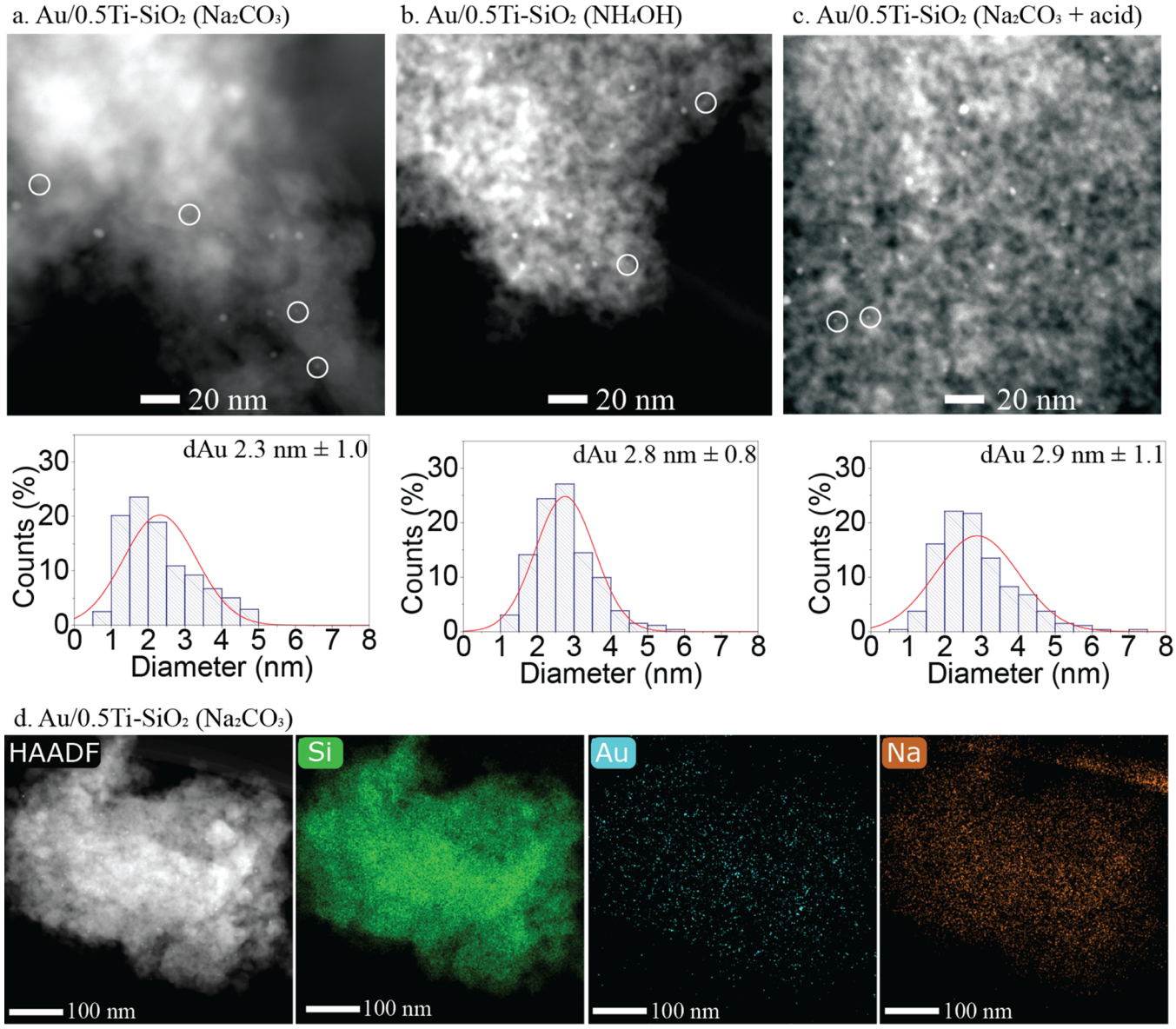

Figure 2. (a−c) HAADF-STEM images of selected 0.2 wt % Au/0.5Ti-SiO_2 catalysts. (d) EDX map of Au/0.5Ti-SiO_2 (Na_2CO_3). Small gold clusters are highlighted by white circles in the HAADF-STEM images.

Reaction products were quantified with a standard gas mixture with known concentrations using an online Interscience Compact GC 4.0 (analysis time 8 min) equipped with a Porabond Q column and a Molsieve 5A column in two separate channels, both with a thermal conductivity detector. The Au/SiO_2 catalyst, without titanium, only produced trace

https://doi.org/10.1021/acs.jpcc.1c05503
J. Phys. Chem. C 2021, 125, 16557−16568

amounts of acrolein and water. The 0.5Ti-SiO_2 that did not contain gold did not show any activity under the studied conditions. Also, Au/xTi-SiO_2 was inactive in propene oxidation at 200 °C in the absence of H_2 in the gas feed. No propene hydrogenation activity was observed for the studied catalysts. The conversion of propene at time i was calculated from the total sum of moles of carbon in the oxygenates (propene oxide, propanal, acetone, acrolein, ethanal, and CO_x) as

$$\chi_{C_3H_6}(\%) = \frac{\sum nC_{\text{oxygenates}_i}}{nC_{\text{feed}_0}} \cdot 100\%$$

The selectivities toward products propene oxide and propanal at reaction time i were calculated as

$$S_{PO}(\%) = \frac{nC_{PO_i}}{\sum nC_{\text{oxygenates}_i}} \cdot 100\%$$

$$S_{PA}(\%) = \frac{nC_{PA_i}}{\sum nC_{\text{oxygenates}_i}} \cdot 100\%$$

The conversion of hydrogen was calculated as

$$\chi_{H_2}(\%) = \frac{nH_{2_i}}{nH_{2_0}} \cdot 100\%$$

RESULTS AND DISCUSSION

Catalyst Characterization. Figure 1a shows the diffuse reflectance UV−vis (DR UV−vis) absorption spectra of silica supports with different loadings of titanium(IV), denoted as xTi-SiO_2, with x indicating the number of titanium atoms/nm^2. The 0.1Ti-SiO_2, with a nominal loading of 0.4 wt % Ti, shows two absorption maxima, at 221 and 252 nm, respectively. These maxima correspond to isolated tetrahedral Ti-OH sites and hydrated isolated Ti-OH sites as reported by García-Aguilar *et al.*[28,29] The absorption maximum of 0.5Ti-SiO_2 at 1.9 wt % Ti shows a red-shift, most likely due to the presence of dimers or small oligomers of TiO_x. For both supports, the absorbance maxima and optical edge energies (see Figures S2−S4) are in good agreement with isolated hydrated Ti-sites, but the oligomerization of Ti-sites for the 0.5Ti-SiO_2 support cannot be ruled out.[12,19,30,31] The X-ray diffractogram (Figure S5) does not contain any diffraction lines that can be ascribed to crystalline TiO_2.

The bifunctional Au catalysts using xTi-SiO_2 as a support (at a nominal Au loading of 0.2 wt %) were prepared via cation adsorption using literature procedures.[19,25,32−37] $Au(en)_2Cl_3$ or $HAuCl_4 \cdot 3H_2O$ was used as a Au precursor at high pH (9.4−9.6) using either Na_2CO_3 or NH_4OH(aq) as a base as indicated. For example, Au/0.1Ti-SiO_2 (Na_2CO_3) stands for the catalyst prepared using Na_2CO_3 as a base. The use of these specific combinations of a gold precursor and base results in catalysts with similar final gold loadings and gold particle sizes. Larger gold nanoparticles were obtained for the combination of $Au(en)_2Cl_3$ and NH_4OH(aq). Meanwhile, it is reported in the literature that deposition precipitation of $HAuCl_4 \cdot 3H_2O$ with alkali bases on Ti-SiO_2 supports suffers from inefficient gold uptake from the precursor solution and therefore results in catalysts with lower gold loadings.

DR UV−vis spectra of gold nanoparticles supported on 0.5Ti-SiO_2 (Figure 1b) and 0.1Ti-SiO_2 (Figure 1c) show that titanium(IV) is still present as isolated hydrated Ti-sites in Au/Ti-SiO_2 along with gold nanoparticles as clear from the localized surface plasmon resonance band located at 510−525 nm.

Figure 2a−c and Figure S8a,b show representative HAADF-STEM images of gold nanoparticles supported on xTi-SiO_2 and their corresponding particle size distribution. Au particles of 2.3 ± 1.0 nm to 2.9 ± 1.1 nm were present, irrespective of the base used during the preparation or the Ti density on the silica support. STEM-EDX (Figure S8c,d) showed small clusters of Ti in the Na_2CO_3-derived Au/0.5Ti-SiO_2, in line with the earlier observation with UV−vis that in this sample, oligomeric TiO_x was present.

Table 1 summarizes the characterization data for both gold-containing catalysts and Ti-SiO_2 at different metal contents and after different treatments. No change in the Ti-loading is observed upon the gold deposition. The acidic properties of the support material and Au/Ti-SiO_2 were determined by mass titration.[38] The pristine silica support showed weak acidic properties with a point-of-zero-charge (PZC) of 5.6. Grafting Ti on the silica surface led to a decrease in the PZC, implying a more acidic character of Ti-OH groups compared to surface silanols. The PZC of the 0.1Ti-SiO_2 support is 2.8 and is lower than that of 0.5Ti-SiO_2 at 3.6. This difference suggests the presence of some oligomeric TiO_x sites at higher titanium(IV) loadings. As indicated by UV−vis, our 0.1Ti-SiO_2 support contains isolated tetrahedral titanium(IV) sites, where one titanium atom is coordinated by four oxygen atoms. As demonstrated by Fois and co-workers, these tetrahedral titanium(IV) sites possess a more acidic character compared to catalysts with octahedral titanium(IV) sites. Here, the titanium center is coordinated by six oxygen atoms, which reduced the acidity, as is the case for oligomeric TiO_x species.[39] FTIR analysis with adsorption and desorption of pyridine showed the presence of Lewis acid sites on 0.5Ti-SiO_2

Table 1. Characterization of Selected Au/xTi-SiO_2 Catalysts[a]

catalyst	Au content (wt %)	Ti content (wt %)	density of Ti-sites (atoms/nm^2)	gold particle size (nm)	PZC
SiO_2					5.6
0.1Ti-SiO_2			(0.10 nominal)		2.8
0.5Ti-SiO_2		1.93	0.49		3.6
Au/0.5Ti-SiO_2 (Na_2CO_3)	0.18	1.84	0.46	2.3 ± 1.0	9.6
Au/0.5Ti-SiO_2 (Na_2CO_3 + acid)	0.19	1.71	0.43	2.9 ± 1.1	4.0
Au/0.1Ti-SiO_2 (Na_2CO_3)	0.16			2.7 ± 0.8	8.4
Au/0.5Ti-SiO_2 (NH_4OH)	0.16	2.01	0.50	2.8 ± 0.8	4.5
Au/0.5Ti-SiO_2 (NH_4OH + base)					10.3
Au/0.1Ti-SiO_2 (NH_4OH)	0.16			3.1 ± 1.2	5.6
Au/SiO_2 (Na_2CO_3)	0.11			2.5 ± 1.0	10.3
Au/SiO_2 (NH_4OH)	0.11			4.2 ± 1.3	5.5

[a]Loadings of Au and Ti were determined by ICP, and the gold particle size was determined by HAADF-STEM.

https://doi.org/10.1021/acs.jpcc.1c05503
J. Phys. Chem. C 2021, 125, 16557−16568

as opposed to the pristine SiO_2 that does not show Lewis acidity (Figure S6).

A clear difference in the materials' PZC is observed for Au-containing catalysts prepared using either Na_2CO_3 or NH_4OH as a base during the gold deposition step. The use of Na_2CO_3 led to a significant increase in the surface basicity compared to the xTi-SiO_2 support. EDX analysis of Au/0.5Ti-SiO_2 (Na_2CO_3) showed that Na is present (Figure 2d and Figure S9a), while the PZC of the catalyst increased to 9.6. In addition, FTIR analysis of the same catalyst (Figure S7) confirmed the presence of sodium carbonate (1421 and 1576 cm^{-1})[40] on the Ti-SiO_2 support surface. Interestingly, no carbonate residues were detected on the SiO_2 surface of the Au/SiO_2 (Na_2CO_3) catalyst in the absence of titanium(IV) (Figure S7). Hence, it is expected that Na^+ neutralizes the acidic Ti-sites and thus neutralizes the acidity of the support, as illustrated in Figure 3. The X-ray photoelectron spectrum of

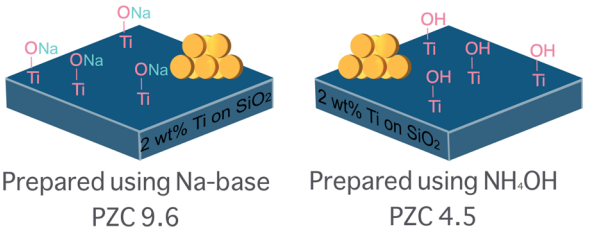

Figure 3. Schematic illustration of the surface sites in Au/Ti-SiO_2 prepared using different bases. (a) Au/Ti-SiO_2 catalyst with Ti-ONa moieties. (b) Au/Ti-SiO_2 catalyst with acidic surface Ti-OH groups.

Na 1s (Figure S11) supports this. It shows the presence of Na^+ on the surface of the Au/SiO_2 and Au/0.5Ti-SiO_2 catalysts that were prepared with Na_2CO_3, while Na^+ is absent for the Au/0.5Ti-SiO_2 catalyst that was prepared with NH_4OH(aq).

For catalysts prepared with dilute ammonium hydroxide as a base during gold deposition (catalysts denoted with NH_4OH), FTIR did not show any NH_3 residues after the thermal treatment (Figure S7). Also, the PZC measurement of these catalysts show preservation of the acidity, in contrast to the Na_2CO_3-derived catalysts, which can be explained by the facile desorption/decomposition of ammonia during calcination. Hence, the use of Na_2CO_3 during gold deposition leads to neutralization of acidic Ti-sites in the Au/xTi−SiO_2 catalyst, while the use of NH_4OH leads to preservation of the surface acidity. Alternatively, a post-synthesis treatment of the neutralized catalyst Au/0.5Ti-SiO_2 (Na_2CO_3) with dilute nitric acid (denoted as Na_2CO_3 + acid) resulted in the removal of Na as observed in the EDX spectrum (Figure S9b) and restoration of the support surface acidity without a major change in the gold particle size.

The oxidation states of Au and Ti were characterized by X-ray photoelectron spectroscopy (XPS) as shown in Figure 4. Figure 4a,c demonstrates the Ti 2p spectra of the catalyst prepared with Na_2CO_3 and NH_4OH(aq), respectively. The intense Ti $2p_{3/2}$ peak at 459.1−459.7 eV agrees with tetrahedral Ti^{4+} species.[41] It is slightly lower compared to Ti^{4+} in titanosilicate-1, indicating that a minor amount of oligomeric TiO_x can be present as previously mentioned.[41,42] No shoulder at lower binding energy corresponding to TiO_2 was observed around 458.3 eV.[43] Figure 4b,d demonstrates the Au 4f spectra. The Au $4f_{7/2}$ peak is observed at 83.7 and 84.0 eV for the Au catalyst prepared with Na_2CO_3 and NH_4OH, respectively, indicating that Au is present in the metallic Au^0

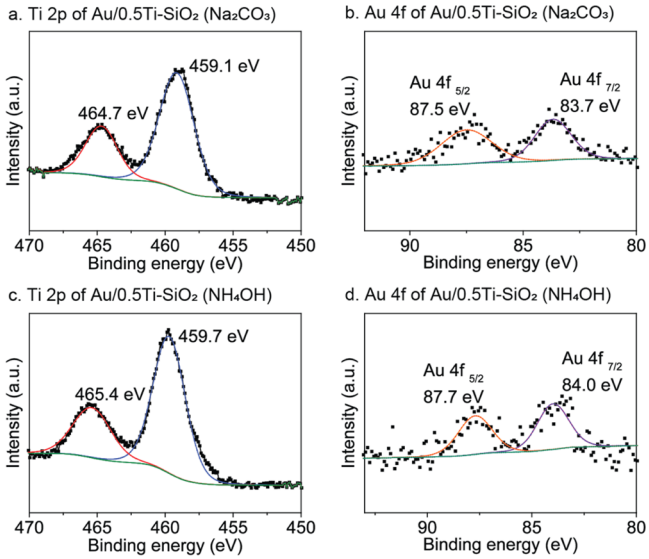

Figure 4. XPS spectra of (a, b) Ti 2p and Au 4f regions of Au/0.5Ti-SiO_2 (Na_2CO_3) and (c, d) of Au/0.5Ti-SiO_2 (NH_4OH).

state in both catalysts.[42,44] The gold catalyst without titanium, Au/SiO_2 (Na_2CO_3), shows a similar binding energy at 84.0 eV. Although the peak intensity is low due to the low gold loading, no shoulder at 84.6 or 86.0 eV was observed corresponding to cationic Au^+ and Au^{3+}, respectively.[44,45]

Selectivity in Catalytic Propene Oxidation with O_2/H_2. Both NH_4OH- and Na_2CO_3-derived Au/0.5Ti-SiO_2 catalysts with a nominal Au-loading of 0.20 wt % were studied in gas-phase propene oxidation with an O_2/H_2 mixture at 200 °C after treatment with 20% H_2 in He at 250 °C. The conversions and selectivity of the Au−Ti bifunctional catalysts are shown in Figure 5.

Clear differences in the performance in propene oxidation are observed for catalysts prepared using different bases (Figure 5). Both Na_2CO_3-derived (blue) and NH_4OH-derived (red) catalysts show propene conversions of 2.2−2.6% (Figure 5a), while the H_2 conversion of the Na_2CO_3-derived catalyst is slightly higher (35.8%) compared to that of the NH_4OH-derived catalysts (19.7%, Figure 5b). Moreover, a significant difference is observed in the product selectivity (Figure 5c,d). The Na_2CO_3-derived catalyst showed a high selectivity toward propene oxide (89.3%, Figure 5c) with trace amounts of other oxygenates, such as ethanal, acrolein, and CO, and almost no propanal. For the Au/0.5Ti-SiO_2 (NH_4OH), propanal formed as the main product with 83.4% selectivity (Figure 5d) and only traces of PO, acrolein, acetone, ethanal, and CO were observed. The average PO formation rate was 48.4 $g_{PO}{\cdot}kg_{cat}^{-1}{\cdot}h^{-1}$ for Au/0.5Ti-SiO_2 (Na_2CO_3), and the average propanal formation rate was 53.4 $g_{propanal}{\cdot}kg_{cat}^{-1}{\cdot}h^{-1}$ for the Au/0.5Ti-SiO_2 (NH_4OH) catalyst, while the H_2 efficiency for both catalysts was typically <11.0% (Table 2). These catalysts are less active than catalysts reported in the literature supported on titanosilicate-1 (TS-1), showing higher PO formation rates of up to 112−137 $g_{PO}{\cdot}kg_{cat}^{-1}{\cdot}h^{-1}$ at 200 °C.[28,46,47] No catalyst has, however, been reported with the high propanal formation rate that we report here; propanal is often only observed in minor amounts for catalysts with lower Ti-content.[19] An overview of reaction rates and hydrogen efficiency is given in Table 2. The best-performing catalyst was recycled (Figure S12) and showed deactivation in propene conversion during

https://doi.org/10.1021/acs.jpcc.1c05503
J. Phys. Chem. C 2021, 125, 16557−16568

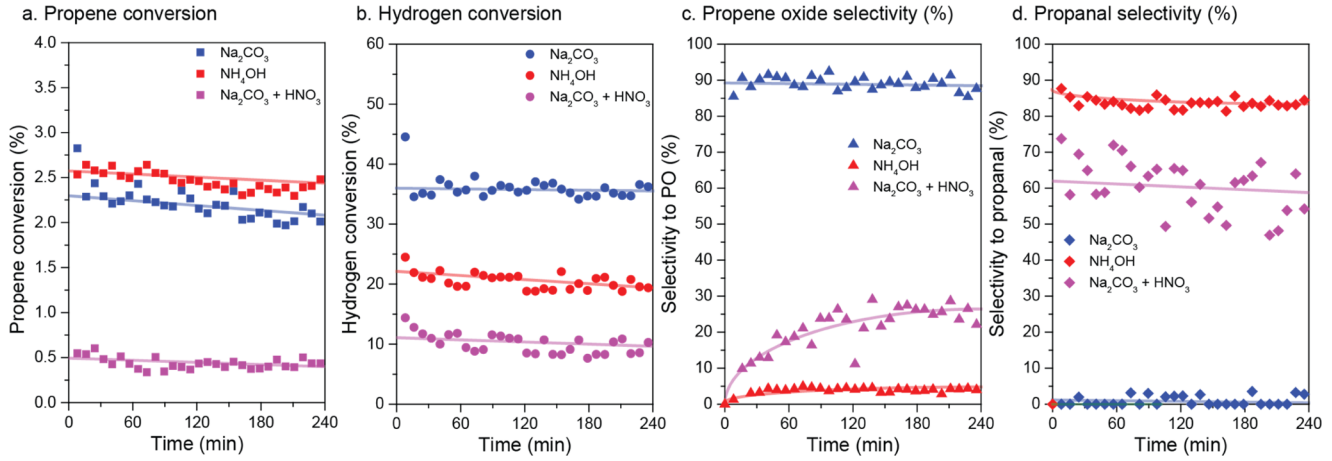

Figure 5. Catalytic behavior of Au/0.5Ti-SiO_2 catalysts in propene oxidation at 200 °C, a flow of 10,000 mL/g_{cat}/h, and a 1/1/1/7 ratio of C_3H_6/O_2/H_2/He. (a) Propene conversion, (b) hydrogen conversion, (c) propene oxide selectivity, and (d) propanal selectivity. The colors indicate the base used for pH control during catalyst preparation. Solid lines are added to guide the eyes.

Table 2. Effect of Ti-Loading and the Preparation Method on Propene Oxidation with O_2/H_2 at 200 °C and a Flow of 10,000 mL/g_{cat}/h

entry	catalyst	χC_3H_6(%)	χH_2(%)	S_{PO} (%)	$S_{propanal}$ (%)	H_2 efficiency[a] (%)	PO formation rate (mol·gcat^{-1}·s^{-1})	propanal formation rate (mol·gcat^{-1}·s^{-1})
1	Au/0.5Ti-SiO_2 (Na_2CO_3)	2.2	35.8	89.3	1.0	4.8	2.3×10^{-7}	2.4×10^{-9}
2	Au/0.1Ti-SiO_2 (Na_2CO_3)	1.1	51.4	86.3	2.6	2.3	1.4×10^{-7}	
3	Au/0.5Ti-SiO_2 (NH_4OH)	2.4	19.7	3.9	83.4	11.0	1.2×10^{-8}	2.6×10^{-7}
4	Au/0.1Ti-SiO_2 (NH_4OH)	2.1	28.4	55.9	31.8	4.5 (7.3)[b]	1.4×10^{-7}	8.9×10^{-8}

[a]H_2 efficiency is defined as $r_{PO}/rH_2 \cdot 100\%$ or $r_{propanal}/rH_2 \cdot 100\%$, respectively. [b]7.3% H_2 efficiency taking both PO and propanal formations into account.

the recycling tests, while H_2 conversion remained similar. The propene conversion decreased from 2.8 to 2.1% during the first 4 h of catalytic propene epoxidation at 200 °C and from 1.9 to 1.6% in the second run of 4 h. The slow deactivation of Ti-SiO_2 catalysts that were prepared by grafting methods has been reported previously by Haruta *et al.* and Moulijn *et al.* and is proposed to be due to the irreversible adsorption of propoxy-species at the epoxidation Ti-sites.[16,48]

While the Au-loading, Au particle size, and Ti-loading were similar for our catalysts, the acidic properties of the catalyst surface differed (Table 1). The Au/0.5Ti-SiO_2 catalyst prepared with Na_2CO_3 has a high PZC of 9.6 and has a high selectivity to PO (Figure 5, blue) in accordance with literature reports.[37,49] The catalyst prepared with NH_4OH, which showed preservation of surface acidity with a PZC of 4.5, showed a high selectivity toward propanal. In the literature, there are just a few examples of Au/Ti-based catalysts with a moderate selectivity to propanal.[11] To the best of our knowledge, there are no reports on Au/Ti-based catalysts with the high selectivity to propanal as the one that we report here.

When Au/0.5Ti-SiO_2 (Na_2CO_3) was treated with dilute nitric acid, its PZC decreased to 4.0 (Table 1) and Na was removed as confirmed by EDX (Figure S9a,b). The resulting catalyst showed an increase in aldehyde selectivity compared to the non-acid washed Au/0.5Ti-SiO_2 (Na_2CO_3); however, propene conversion decreased to 0.40% (Figure 5, lilac). The low conversion of propene is possibly the result of Au particle growth caused by the acid treatment from 2.3 ± 1.0 nm to 2.9 ± 1.1 nm. Similarly, impregnating the Au/0.5Ti-SiO_2 (NH_4OH) catalyst with 0.4 wt % NaOH to increase the PZC led to complete inhibition of propene oxidation activity.

Identification of the PO Isomerization Sites. Our results clearly demonstrate that acidic Au/Ti-based catalysts produce propanal as the main product, while catalysts with a high PZC show high selectivities to propene oxide. Interestingly, in the literature, propanal is often observed as a byproduct in trace amounts from propene oxidation.[50,51]

As first suggested by Moulijn *et al.*,[16] acidic surface groups (Ti-OH or Si-OH) convert small amounts of the propene oxide product into propanal, which is irreversibly adsorbed on acidic Ti-OHs, whereas an excess of base residues (ammonium ions and magnesia) at the surface was shown to enhance selectivity toward acetone.[21,52] These suggestions in propene oxidation are similar to observations in ethene oxidation over supported silver catalysts. There, ethene oxide (EO) is converted rapidly over the surface groups of most oxides, such as Si−OH, Al−OH, and Ti−OH.[53−56] Strategies to limit the EO isomerization to ethanal (acetaldehyde) are focused on limiting the amount of surface groups. Therefore, low surface area α-alumina is often reported as the superior support for silver catalysts.[55] Also, in ethene oxidation, alkali addition is used to neutralize surface acidity.[53,57] However, this is the first time that the role of alkali promotors in the surface acidity is reported for propene epoxidation.

https://doi.org/10.1021/acs.jpcc.1c05503
J. Phys. Chem. C 2021, 125, 16557−16568

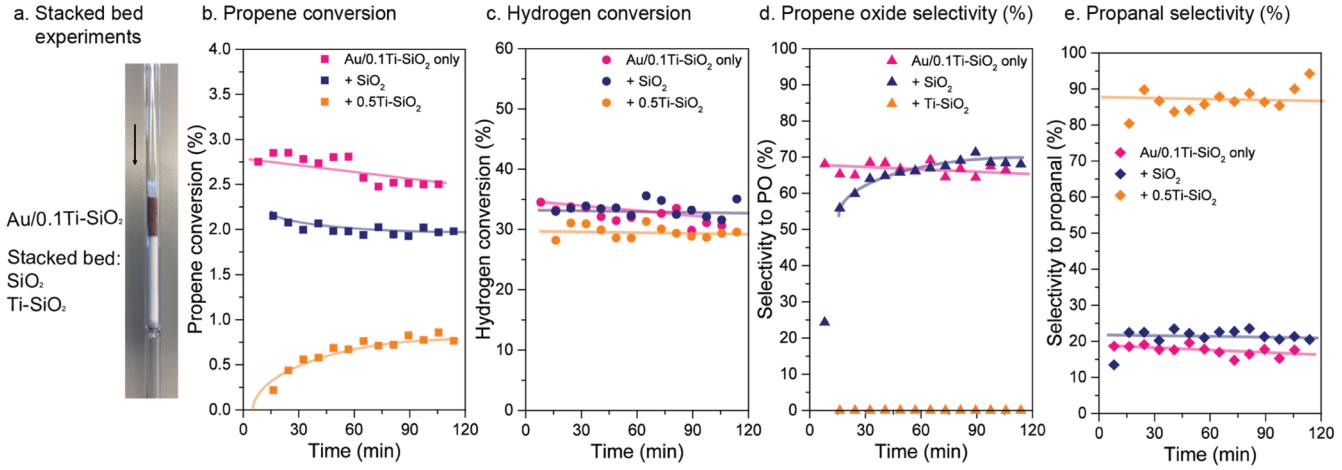

Figure 6. Catalytic results of stacked bed experiments where the Au/Ti-SiO_2 catalyst prepared according to ref 19 was always used as a PO-producing top layer and different support materials were used beneath to study PO isomerization. (a) Example of the loaded reactor tube used for the experiments. (b) Observed propene conversion, (c) observed hydrogen conversion, (d) observed propene oxide selectivity, and (e) observed propanal selectivity. Solid lines are added to guide the eye. Conditions: temperature of 200 °C, flow of 10,000 mL/g_{cat}/h, 1/1/1/7 ratio of C_3H_6/O_2/H_2/He.

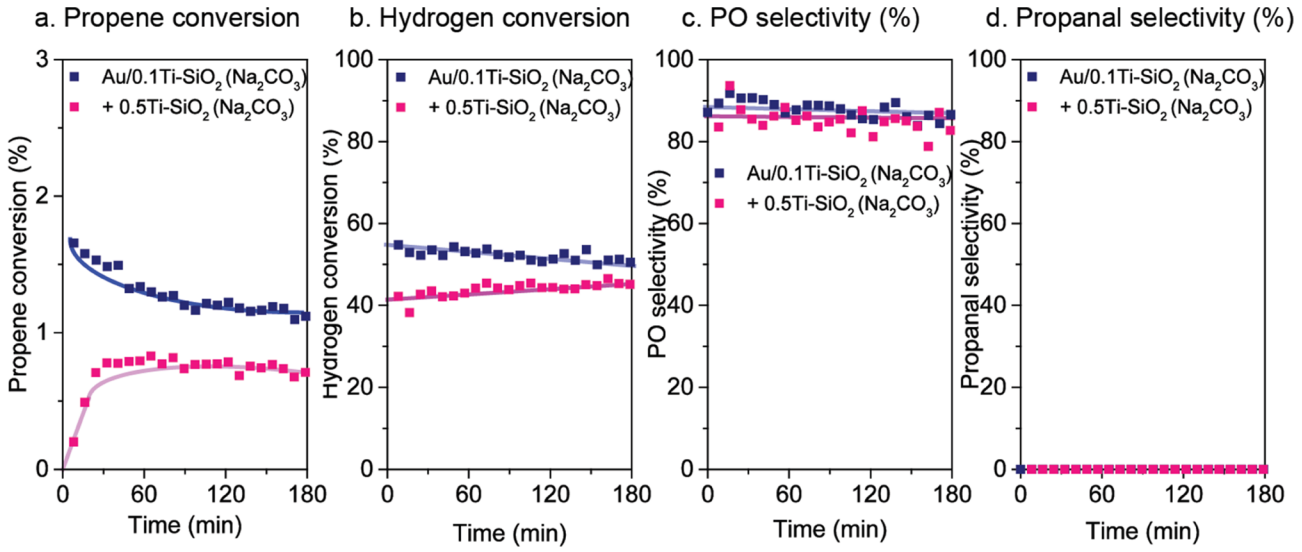

Figure 7. Catalytic results of stacked bed experiments where the Au/0.1Ti-SiO_2 (Na_2CO_3) catalyst was used as a PO-producing top layer and different support materials were used beneath to study PO isomerization. (a) Observed propene conversion, (b) observed hydrogen conversion, (c) observed propene oxide selectivity, and (d) observed propanal selectivity. Solid lines are added to guide the eye. Conditions: temperature of 200 °C, flow of 10,000 mL/g_{cat}/h, 1/1/1/7 ratio of C_3H_6/O_2/H_2/He.

To elucidate whether the observed propanal formed as an intrinsic reaction product in propene oxidation over acidic Au/Ti-SiO_2 or as a product from propene oxide isomerization, we performed stacked bed experiments where the acidic Ti-SiO_2 support was exposed to a gas feed comprising propene oxide.

The Au/0.1Ti-SiO_2 catalyst prepared using a literature procedure[19] and selective toward propene oxide was placed on top of a layer of SiO_2 or 0.5Ti-SiO_2 supports (Figure 6a), using a downward flow of the reactant mixture. The SiO_2 and 0.5Ti-SiO_2 supports alone show no activity in propene oxidation. The propene oxide-producing catalyst (Figure 6, pink) showed a propene conversion of 2.8%, a H_2 conversion of 33.0%, and selectivities of 66.9% toward propene oxide and 18.5% toward propanal. When a pristine SiO_2 bed layer was placed below a Au/0.1Ti-SiO_2 bed, no change in reaction selectivity was observed (Figure 6d,e, blue). On the contrary, when a 0.5Ti-SiO_2 bed was placed beneath the PO-producing catalyst (Figure 6, orange), a complete change in selectivity was observed with no PO formed and propanal becoming the main product (>90%), while TGA-MS confirmed the deposition of carbonaceous species on the exposed 0.5Ti-SiO_2 (Figure S10), explaining the lower propene conversion. We therefore conclude that propanal is formed via isomerization of propene oxide over acidic Ti-sites and not over acidic silanols. This is rather remarkable since EO isomerization has been reported to occur over most acidic surface groups, both including Si-OH and Ti-OH.[55] Yet, here, we observe that PO isomerization requires the Lewis acidic Ti-sites of the Ti-containing support as catalytic centers. Similar to ethene oxidation, these acidic sites can be neutralized by an alkali base. Catalysts producing larger amounts of propanal were reported before, but no relation with the alkali base was mentioned. For instance, Haruta *et al.* observed propanal with 74% selectivity at 0.6% propene conversion as the product from propene epoxidation

https://doi.org/10.1021/acs.jpcc.1c05503
J. Phys. Chem. C 2021, 125, 16557−16568

using an "extensively" washed Au/TS-1 catalyst. This is the highest propanal yield reported so far.[11] Their observation might be due to the removal of alkali during washing since later Au/TS-1 catalysts with outstanding PO selectivity were reported.[50,58] Also, catalysts prepared using a non-alkali base, such as NH_4OH, tend to show a higher propanal selectivity.[19] Although no data is reported on the surface acidity of these, the catalysts prepared at elevated pH, using alkali salts, are expected to contain neutralized Ti-sites and hence give high PO selectivity.

Figure 7 shows the catalytic results from a stacked bed experiment where the 0.5Ti-SiO_2 was treated with Na_2CO_3 and tested in the PO isomerization reaction. Both propene (Figure 7a) and hydrogen (Figure 7b) conversions were slightly lower for the stacked bed compared to solely the PO-producing catalyst Au/0.1Ti−SiO_2 (Na_2CO_3). Strikingly, the PO selectivity was 86% for both catalysts (Figure 7c), while no propanal was observed in the effluent gas (Figure 7d). The inhibition of PO isomerization was only observed when Na^+ was present on the catalyst support.

Shown in Scheme 3 are the various products that can be obtained from propene oxidation. Acrolein formation (top pathway) was only observed for the Au/SiO_2 catalyst, without titanium. In the literature, acrolein formation is well reported over mixed metal oxide catalysts,[59] gold catalysts that do not produce propene oxide,[22,60] and supported copper and silver catalysts.[61,62] In the middle is shown the complete oxidation of propene, which is reported for gold and other noble metal catalysts supported on ceria.[45] Propene oxide formation (bottom pathway) is observed for the Au/Ti-SiO_2 (Na_2CO_3) catalyst and many catalysts reported in the literature. In addition, the propene oxide isomerization toward propanal over the used Ti-SiO_2 support is included in the scheme. The isomerization of epoxides to aldehydes is known to be catalyzed by both Lewis and Brønsted acids in organic synthetic chemistry, a reaction known as Meinwald rearrangement.[63,64] To the best of our knowledge, no examples on the heterogeneously catalyzed Meinwald rearrangement of PO to propanal have been reported. As demonstrated here (Scheme 3), PO can be selectively rearranged to propanal by the Ti-OH sites of the Ti-support. Also, as we observed in our stacked bed experiments, these acidic sites are neutralized by the alkali base used during catalyst preparation.

Scheme 3. Overview of Possible Propene Oxidation Pathways

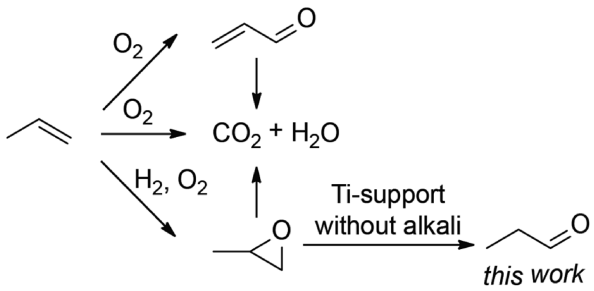

Effect of Ti-Loading on Propene Oxidation. While the results above states that the base used during gold deposition highly affects the selectivity in propene oxidation, Nijhuis *et al.* demonstrated that lowering the Ti-content can be beneficial for PO selectivity for catalysts prepared using NH_4OH.[19] This was supported by Haruta *et al.*, who also showed improved PO selectivity for catalysts with a lower Ti-content, although it is attributed to the lack of Ti-O-Ti oligomers.[65] Since the acidic Ti-sites were responsible for lowering the PO selectivity, we synthesized and studied Au catalysts with a lower Ti-loading (0.1 Ti/nm^2 instead of 0.5 Ti/nm^2). The characterization data are shown in Table 1, and the catalytic results are shown below in Table 2.

The Au/Ti-SiO_2 catalysts prepared with NH_4OH and Na_2CO_3 and different Ti-loadings show similar propene conversions. Catalysts prepared using Na_2CO_3 (entries 1 and 2) both showed a high selectivity toward PO. The lower propene conversion for the catalyst with lower Ti-loading is most likely due to the lack of intimacy between the gold nanoparticles and Ti-sites on the support. This explanation is supported by the increase in H_2 conversion at lower Ti-loadings since without access to the epoxidation Ti-sites, the formed hydroperoxo-species are converted into water.

For the acidic NH_4OH-derived catalysts at high Ti-loading (0.5Ti-SiO_2 as the support, entry 3), propanal was the major product. By lowering the Ti-content, the selectivity changed to a mixture of PO and propanal (entry 4), indicating that there are less Ti-sites available for the rearrangement of PO to propanal. These results clearly indicate that the epoxidation activity of the studied catalyst is unchanged by lowering the Ti-loading while the rearrangement of PO to propanal is changed.

CONCLUSIONS

In this work, we highlight the origin of the isomerization of propene oxide during propene epoxidation over supported gold−titanium(IV) catalysts. We show that acidic Ti-sites of the Ti-SiO_2 support material catalyze the isomerization of PO toward propanal, thus reducing the PO selectivity of catalysts prepared using Ti-SiO_2-based supports, which is undesired. The isomerization activity is completely inhibited by the presence of Na^+ on the Ti-SiO_2 support. Similarly, during gold adsorption, the use of Na^+ bases results in residual Na^+ and neutralized Ti-sites on the final Au/Ti-SiO_2 catalysts. These catalysts were shown to demonstrate high PO selectivity in line with previous reports. Alternatively, the use of NH_4OH shows preservation of acidic sites and the absence of Na^+ in the Au/Ti-SiO_2(NH_4OH) catalysts. During propene epoxidation, these catalysts show unprecedentedly high selectivity toward propanal at a similar propene conversion.

We demonstrate that the (acidic) Ti-OH sites of the support and not the Si-OH sites are responsible for the rearrangement of PO to propanal, leading to the observed difference in selectivity and that these sites are neutralized by the Na^+ base used. Lowering the Ti-loading also limits the PO isomerization to propanal over the studied catalysts. These insights provide guidelines for designing catalysts with tunable selectivity in the oxidation of propene.

ASSOCIATED CONTENT

Supporting Information

The Supporting Information is available free of charge at https://pubs.acs.org/doi/10.1021/acs.jpcc.1c05503.

Physisorption data, DR UV−vis data, XRD, Py-FTIR, additional STEM micrographs, EDS spectra, TGA-MS, additional XPS spectra, and additional catalysis data (PDF)

https://doi.org/10.1021/acs.jpcc.1c05503
J. Phys. Chem. C 2021, 125, 16557−16568

AUTHOR INFORMATION

Corresponding Author

Baira Donoeva − *Materials Chemistry and Catalysis, Debye Institute for Nanomaterials Science, Utrecht University, Utrecht 3584CG, The Netherlands;* Present Address: Present address: Shell Technology Centre Amsterdam, Amsterdam 1031 HW, The Netherlands (B.D.); orcid.org/0000-0002-1702-8857; Email: baira.donoeva@gmail.com

Authors

Ewoud J.J. de Boed − *Materials Chemistry and Catalysis, Debye Institute for Nanomaterials Science, Utrecht University, Utrecht 3584CG, The Netherlands*

Jan Willem de Rijk − *Materials Chemistry and Catalysis, Debye Institute for Nanomaterials Science, Utrecht University, Utrecht 3584CG, The Netherlands*

Petra E. de Jongh − *Materials Chemistry and Catalysis, Debye Institute for Nanomaterials Science, Utrecht University, Utrecht 3584CG, The Netherlands;* orcid.org/0000-0002-2216-2620

Complete contact information is available at: https://pubs.acs.org/10.1021/acs.jpcc.1c05503

Notes

The authors declare no competing financial interest.

ACKNOWLEDGMENTS

The authors acknowledge funding from Utrecht University. The authors would like to thank Petra Keijzer and Lars van der Wal for the electron microscopy images of the prepared materials, Dennie Wezendonk for performing TGA-MS, Pascal Wijten for helping with GC, and Nikos Nikolopoulos for N_2 physisorption, and Petra Keijzer is also thanked for the fruitful discussions. Dr. Nikolay Kosinov (Technical University Eindhoven) is acknowledged for the XPS measurements.

REFERENCES

(1) Grasselli, R. K. Selective Oxidation and Ammoxidation of Olefins by Heterogeneous Catalysis. *J. Chem. Educ.* **1986**, *63*, 216−221.

(2) *Petrochemicals in action*; https://www.petrochemistry.eu (accessed 28 August 2020)

(3) Nijhuis, T. A.; Makkee, M.; Moulijn, J. A.; Weckhuysen, B. M. The Production of Propene Oxide: Catalytic Processes and Recent Developments. *Ind. Eng. Chem. Res.* **2006**, *45*, 3447−3459.

(4) Khatib, S. J.; Oyama, S. T. Direct Oxidation of Propylene to Propylene Oxide with Molecular Oxygen: A Review. *Catal. Rev.* **2015**, *57*, 306−344.

(5) Trent, D. L. Propylene Oxide. In *Kirk-Othmer Encyclopedia of Chemical Technology*; Wiley: New York, 2001.

(6) Sheldon, R. A.; van Doorn, J. A. Metal-Catalyzed Epoxidation of Olefins with Organic Hydroperoxides. I. A Comparison of Various Metal Catalysts. *J. Catal.* **1973**, *31*, 427−437.

(7) Sheldon, R. A.; Wallau, M.; Arends, I. W. C. E.; Schuchardt, U. Heterogeneous Catalysts for Liquid-Phase Oxidations: Philosophers' Stones or Trojan Horses? *Acc. Chem. Res.* **1998**, *31*, 485−493.

(8) Navidi, N.; Thybaut, J. W.; Marin, G. B. Experimental Investigation of Ethylene Hydroformylation to Propanal on Rh and Co Based Catalysts. *Appl. Catal. A Gen.* **2014**, *469*, 357−366.

(9) Hanaoka, T.; Arakawa, H.; Matsuzaki, T.; Sugi, Y.; Kanno, K.; Abe, Y. Ethylene Hydroformylation and Carbon Monoxide Hydrogenation over Modified and Unmodified Silica Supported Rhodium Catalysts. *Catal. Today* **2000**, *58*, 271−280.

(10) Hayashi, T.; Tanaka, K.; Haruta, M. Selective Vapor-Phase Epoxidation of Propylene over Au/TiO_2Catalysts in the Presence of Oxygen and Hydrogen. *J. Catal.* **1998**, *178*, 566−575.

(11) Haruta, M.; Uphade, B. S.; Tsubota, S.; Miyamoto, A. Selective Oxidation of Propylene over Gold Deposited on Titanium-Based Oxides. *Res. Chem. Intermed.* **1998**, *24*, 329−336.

(12) Bravo-Suárez, J. J.; Bando, K. K.; Lu, J.; Haruta, M.; Fujitani, T.; Oyama, T. Transient Technique for Identification of True Reaction Intermediates: Hydroperoxide Species in Propylene Epoxidation on Gold/Titanosilicate Catalysts by X-Ray Absorption Fine Structure Spectroscopy. *J. Phys. Chem. C* **2008**, *112*, 1115−1123.

(13) Green, I. X.; Tang, W.; Neurock, M.; Yates, J. T., Jr. Insights into Catalytic Oxidation at the Au/TiO_2 Dual Perimeter Sites. *Acc. Chem. Res.* **2014**, *47*, 805−815.

(14) Lu, J.; Zhang, X.; Bravo-Suárez, J. J.; Tsubota, S.; Gaudet, J.; Oyama, S. T. Kinetics of Propylene Epoxidation Using H_2 and O_2 over a Gold/Mesoporous Titanosilicate Catalyst. *Catal. Today* **2007**, *123*, 189−197.

(15) Harris, J. W.; Arvay, J.; Mitchell, G.; Delgass, W. N.; Ribeiro, F. H. Propylene Oxide Inhibits Propylene Epoxidation over Au/TS-1. *J. Catal.* **2018**, *365*, 105−114.

(16) Mul, G.; Zwijnenburg, A.; van der Linden, B.; Makkee, M.; Moulijn, J. A. Stability and Selectivity of Au/TiO_2 and $Au/TiO_2/SiO_2$ Catalysts in Propene Epoxidation: An in Situ FT-IR Study. *J. Catal.* **2001**, *201*, 128−137.

(17) Ruiz, A.; van der Linden, B.; Makkee, M.; Mul, G. Acrylate and Propoxy-Groups: Contributors to Deactivation of Au/TiO2 in the Epoxidation of Propene. *J. Catal.* **2009**, *266*, 286−290.

(18) Kalvachev, Y. A.; Hayashi, T.; Tsubota, S.; Haruta, M. Vapor-Phase Selective Oxidation of Aliphatic Hydrocarbons over Gold Deposited on Mesoporous Titanium Silicates in the Co-Presence of Oxygen and Hydrogen. *J. Catal.* **1999**, *186*, 228−233.

(19) Chen, J.; Halin, S. J. A.; Pidko, E. A.; Verhoeven, M. W. G. M. T.; Ferrandez, D. M. P.; Hensen, E. J. M.; Schouten, J. C.; Nijhuis, T. A. Enhancement of Catalyst Performance in the Direct Propene Epoxidation: A Study into Gold-Titanium Synergy. *ChemCatChem* **2013**, *5*, 467−478.

(20) Qi, C.; Huang, J.; Bao, S.; Su, H.; Akita, T.; Haruta, M. Switching of Reactions between Hydrogenation and Epoxidation of Propene over Au/Ti-Based Oxides in the Presence of H_2 and O_2. *J. Catal.* **2011**, *281*, 12−20.

(21) Stangland, E. E.; Taylor, B.; Andres, R. P.; Delgass, W. N. Direct Vapor Phase Propylene Epoxidation over Deposition-Precipitation Gold-Titania Catalysts in the Presence of H_2/O_2 : Effects of Support, Neutralizing Agent, and Pretreatment. *J. Phys. Chem. B* **2005**, *109*, 2321−2330.

(22) Huang, J.; Takei, T.; Ohashi, H.; Haruta, M. Propene Epoxidation with Oxygen over Gold Clusters: Role of Basic Salts and Hydroxides of Alkalis. *Appl. Catal. A Gen.* **2012**, *435-436*, 115−122.

(23) Perez Ferrandez, D. M.; Herguedas Fernandez, I.; Teley, M. P. G.; de Croon, M. H. J. M.; Schouten, J. C.; Nijhuis, T. A. Kinetic Study of the Selective Oxidation of Propene with O_2 over Au−Ti Catalysts in the Presence of Water. *J. Catal.* **2015**, *330*, 396−405.

(24) Maschmeyer, T.; Rey, F.; Sankar, G.; Thomas, J. M. Heterogeneous Catalysts Obtained by Grafting Metallocene Complexes onto Mesoporous Silica. *Nature* **1995**, *378*, 159−162.

(25) Zhu, H.; Liang, C.; Yan, W.; Overbury, S. H.; Dai, S. Preparation of Highly Active Silica-Supported Au Catalysts for Co Oxidation by a Solution-Based Technique. *J. Phys. Chem. B* **2006**, *110*, 10842−10848.

(26) Block, B. P.; Bailar, J. C., Jr. The Reaction of Gold(III) with Some Bidentate Cordinating Groups. *J. Am. Chem. Soc.* **1951**, *73*, 4722−4725.

(27) Emeis, C. A. Determination of Integrated Molar Extinction Coefficients for Infrared Absorption Bands of Pyridine Adsorbed on Solid Acid Catalysts. *J. Catal.* **1993**, 347.

(28) García-Aguilar, J.; Fernández-Catalá, J.; Juan-Juan, J.; Such-Basáñez, I.; Chinchilla, L. E.; Calvino-Gámez, J. J.; Cazorla-Amorós,

D.; Berenguer-Murcia, Á. Novelty without Nobility: Outstanding Ni/Ti-SiO_2 Catalysts for Propylene Epoxidation. *J. Catal.* **2020**, *386*, 94−105.
(29) García-Aguilar, J.; Navlani-García, M.; Berenguer-Murcia, Á.; Mori, K.; Kuwahara, Y.; Yamashita, H.; Cazorla-Amorós, D. Enhanced Ammonia-Borane Decomposition by Synergistic Catalysis Using CoPd Nanoparticles Supported on Titano-Silicates. *RSC Adv.* **2016**, *6*, 91768−91772.
(30) Geobaldo, F.; Bordiga, S.; Zecchina, A.; Giamello, E.; Leofanti, G.; Petrini, G. DRS UV-Vis and EPR Spectroscopy of Hydroperoxo and Superoxo Complexes in Titanium Silicalite. *Catal. Letters* **1992**, *16*, 109−115.
(31) Eaton, T. R.; Boston, A. M.; Thompson, A. B.; Gray, K. A.; Notestein, J. M. Counting Active Sites on Titanium Oxide-Silica Catalysts for Hydrogen Peroxide Activation through in Situ Poisoning with Phenylphosphonic Acid. *ChemCatChem* **2014**, *6*, 3215−3222.
(32) Lu, Z.; Piernavieja-Hermida, M.; Turner, C. H.; Wu, Z.; Lei, Y. Effects of TiO_2 in Low Temperature Propylene Epoxidation Using Gold Catalysts. *J. Phys. Chem. C* **2018**, *122*, 1688.
(33) Nijhuis, T. A.; Huizinga, B. J.; Makkee, M.; Moulijn, J. A. Direct Epoxidation of Propene Using Gold Dispersed on TS-1 and Other Titanium-Containing Supports. *Ind. Eng. Chem. Res.* **1999**, *38*, 884−891.
(34) Zanella, R.; Giorgio, S.; Henry, C. R.; Louis, C. Alternative Methods for the Preparation of Gold Nanoparticles Supported on TiO_2. *J. Phys. Chem. B* **2002**, *106*, 7634−7642.
(35) Zanella, R.; Louis, C. Influence of the Conditions of Thermal Treatments and of Storage on the Size of the Gold Particles in Au/TiO_2 Samples. *Catal. Today* **2005**, *107-108*, 768−777.
(36) Zanella, R.; Delannoy, L.; Louis, C. Mechanism of Deposition of Gold Precursors onto TiO_2 during the Preparation by Cation Adsorption and Deposition-Precipitation with NaOH and Urea. *Appl. Catal. A Gen.* **2005**, *291*, 62−72.
(37) Lee, W. S.; Cem Akatay, M.; Stach, E. A.; Ribeiro, F. H.; Nicholas Delgass, W. Reproducible Preparation of Au/TS-1 with High Reaction Rate for Gas Phase Epoxidation of Propylene. *J. Catal.* **2012**, *287*, 178−189.
(38) Ẑalac, S.; Kallay, N. Application of Mass Titration to the Point of Zero Charge Determination. *J. Colloid Interface Sci.* **1992**, *149*, 233−240.
(39) Spanó, E.; Tabacchi, G.; Gamba, A.; Fois, E. On the Role of Ti(IV) as a Lewis Acid in the Chemistry of Titanium Zeolites: Formation, Structure, Reactivity, and Aging of Ti-Peroxo Oxidizing Intermediates. A First Principles Study. *J. Phys. Chem. B* **2006**, *110*, 21651−21661.
(40) Mino, L.; Spoto, G.; Ferrari, A. M. CO_2 Capture by TiO_2 Anatase Surfaces: A Combined DFT and FTIR Study. *J. Phys. Chem. C* **2014**, *118*, 25016−25026.
(41) Capel-Sanchez, M. C.; Campos-Martin, J. M.; Fierro, J. L. G. Impregnation Treatments of TS-1 Catalysts and Their Relevance in Alkene Epoxidation with Hydrogen Peroxide. *Appl. Catal. A Gen.* **2003**, *246*, 69−77.
(42) Chen, X. Y.; Chen, S. L.; Jia, A. P.; Lu, J. Q.; Huang, W. X. Gas Phase Propylene Epoxidation over Au Supported on Titanosilicates with Different Ti Chemical Environments. *Appl. Surf. Sci.* **2017**, *393*, 11−22.
(43) Erdem, B.; Hunsicker, R. A.; Simmons, G. W.; Sudol, E. D.; Dimonie, V. L.; El-Aasser, M. S. XPS and FTIR Surface Characterization of TiO_2 Particles Used in Polymer Encapsulation. *Langmuir* **2001**, *17*, 2664−2669.
(44) Karpenko, A.; Leppelt, R.; Plzak, V.; Behm, R. J. The Role of Cationic Au3+ and Nonionic Au0 Species in the Low-Temperature Water-Gas Shift Reaction on Au/CeO_2 Catalysts. *J. Catal.* **2007**, *252*, 231−242.
(45) Delannoy, L.; Fajerwerg, K.; Lakshmanan, P.; Potvin, C.; Méthivier, C.; Louis, C. Supported Gold Catalysts for the Decomposition of VOC: Total Oxidation of Propene in Low Concentration as Model Reaction. *Appl. Catal. B Environ.* **2010**, *94*, 117−124.
(46) Taylor, B.; Lauterbach, J.; Delgass, W. N. Gas-Phase Epoxidation of Propylene over Small Gold Ensembles on TS-1. *Appl. Catal. A Gen.* **2005**, *291*, 188−198.
(47) Huang, J.; Takei, T.; Akita, T.; Ohashi, H.; Haruta, M. Gold Clusters Supported on Alkaline Treated TS-1 for Highly Efficient Propene Epoxidation with O_2 and H_2. *Appl. Catal. B Environ.* **2010**, *95*, 430−438.
(48) Sinha, A. K.; Seelan, S.; Akita, T.; Tsubota, S.; Haruta, M. Vapor Phase Propylene Epoxidation over Au/Ti-MCM-41 Catalysts Prepared by Different Ti Incorporation Modes. *Appl. Catal. A Gen.* **2003**, *240*, 243−252.
(49) Feng, X.; Yang, J.; Duan, X.; Cao, Y.; Chen, B.; Chen, W.; Lin, D.; Qian, G.; Chen, D.; Yang, C.; Zhou, X. Enhanced Catalytic Performance for Propene Epoxidation with H_2 and O_2 over Bimetallic Au−Ag/Uncalcined Titanium Silicate-1 Catalysts. *ACS Catal.* **2018**, *8*, 7799−7808.
(50) Stangland, E. E.; Stavens, K. B.; Andres, R. P.; Delgass, W. N. Characterization of Gold-Titania Catalysts via Oxidation of Propylene to Propylene Oxide. *J. Catal.* **2000**, *191*, 332−347.
(51) Kanungo, S.; Keshri, K. S.; van Hoof, A. J. F.; d'Angelo, M. F. N.; Schouten, J. C.; Nijhuis, T. A.; Hensen, E. J. M.; Chowdhury, B. Silylation Enhances the Performance of Au/Ti-SiO_2 catalysts in Direct Epoxidation of Propene Using H_2 and O_2. *J. Catal.* **2016**, *344*, 434−444.
(52) Okamoto, Y.; Imanaka, T.; Teranishi, S. The Isomerization of Propylene Oxide on Metal Oxides and Silica-Magnesia Catalysts. *Bull. Chem. Soc. Jpn.* **1973**, *46*, 4−8.
(53) Mao, C.-F.; Albert Vannice, M. High Surface Area α-Aluminas III. Oxidation of Ethylene, Ethylene Oxide, and Acetaldehyde over Silver Dispersed on High Surface Area α-Alumina. *Appl. Catal. A Gen.* **1995**, *122*, 61−76.
(54) Bulushev, D. A.; Paukshtis, E. A.; Nogin, Y. N.; Bal'zhinimaev, B. S. Transient Response and Infrared Studies of Ethylene Oxide Reactions on Silver Catalysts and Supports. *Appl. Catal. A Gen.* **1995**, *123*, 301−322.
(55) van den Reijen, J. E.; Versluis, W. C.; Kanungo, S.; d'Angelo, M. F.; de Jong, K. P.; de Jongh, P. E. From Qualitative to Quantitative Understanding of Support Effects on the Selectivity in Silver Catalyzed Ethylene Epoxidation. *Catal. Today* **2019**, *338*, 31.
(56) Yong, Y.-S.; Kennedy, E. M.; Cant, N. W. Oxide Catalysed Reactions of Ethylene Oxide under Conditions Relevant to Ethylene Epoxidation over Supported Silver. *Appl. Catal.* **1991**, *76*, 31−48.
(57) Nielsen, R. P.; La Rochelle, J. H. Catalyst for production of ethylene oxide. US 3,962,136A, 1975.
(58) Huang, J.; Lima, E.; Akita, T.; Guzmán, A.; Qi, C.; Takei, T.; Haruta, M. Propene Epoxidation with O_2 and H_2: Identification of the Most Active Gold Clusters. *J. Catal.* **2011**, *278*, 8−15.
(59) Sprenger, P.; Kleist, W.; Grunwaldt, J. D. Recent Advances in Selective Propylene Oxidation over Bismuth Molybdate Based Catalysts: Synthetic, Spectroscopic, and Theoretical Approaches. *ACS Catal.* **2017**, *7*, 5628−5642.
(60) Suo, Z.; Jin, M.; Lu, J.; Wei, Z.; Li, C. Direct Gas-Phase Epoxidation of Propylene to Propylene Oxide Using Air as Oxidant on Supported Gold Catalyst. *J. Nat. Gas Chem.* **2008**, *17*, 184−190.
(61) Reitz, J. B.; Solomon, E. I. Propylene Oxidation on Copper Oxide Surfaces: Electronic and Geometric Contributions to Reactivity and Selectivity. *J. Am. Chem. Soc.* **1998**, *120*, 11467−11478.
(62) Teržan, J.; Huš, M.; Likozar, B.; Djinović, P. Propylene Epoxidation Using Molecular Oxygen over Copper-and Silver-Based Catalysts: A Review. *ACS Catal.* **2020**, *10*, 13415−13436.
(63) Robinson, M. W. C.; Pillinger, K. S.; Graham, A. E. Highly Efficient Meinwald Rearrangement Reactions of Epoxides Catalyzed by Copper Tetrafluoroborate. *Tetrahedron Lett.* **2006**, *47*, 5919−5921.
(64) Umeda, R.; Muraki, M.; Nakamura, Y.; Tanaka, T.; Kamiguchi, K.; Nishiyama, Y. Rhenium Complex-Catalyzed Meinwald Rearrangement Reactions of Oxiranes. *Tetrahedron Lett.* **2017**, *58*, 2393−2395.
(65) Uphade, B. S.; Yamada, Y.; Akita, T.; Nakamura, T.; Haruta, M. Synthesis and Characterization of Ti-MCM-41 and Vapor-Phase

https://doi.org/10.1021/acs.jpcc.1c05503
J. Phys. Chem. C 2021, 125, 16557−16568

Epoxidation of Propylene Using H_2 and O_2 over Au/Ti-MCM-41. *Appl. Catal. A Gen.* **2001**, *215*, 137−148.

https://doi.org/10.1021/acs.jpcc.1c05503
J. Phys. Chem. C 2021, 125, 16557−16568